

Single Gold Nanoparticles Encapsulated in Monodispersed Regular Spheres of Mesostructured Silica Produced by Pseudomorphic Transformation

Pablo Botella,* Avelino Corma,* and María Teresa Navarro

Instituto de Tecnología Química, UPV-CSIC, Avda. Los Naranjos s/n, 46022 Valencia, Spain

Received December 12, 2006. Revised Manuscript Received January 29, 2007

Monodispersed, uniform, gold encapsulated–mesoporous silica nanocomposites of 100–350 nm diameter with a centered metal core at about 15 or 30 nm and high gold occupancy are prepared by pseudomorphic transformation of preformed gold–silica nanospheres. The characterization by X-ray powder diffraction, transmission electron microscopy, ^{29}Si and ^{13}C magic angle spinning NMR, and N_2 adsorption isotherms indicates that these materials present the same morphology and particle size distribution of the parent amorphous silica but with an ordered mesoporous shell of complex wormhole-like pore structure and specific surface area of about $1000 \text{ m}^2 \text{ g}^{-1}$. This method is particularly advantageous for both stabilizing gold nanoparticles and tailoring structural and textural parameters of the outer shell, thus, offering an exceptional support for particle functionalization.

Introduction

Gold nanoparticles (GNP) are nowadays the subject of a wide field of research because of the behavior of individual nanoparticles, quantum-size effect, and applications in catalysis and biology.^{1–6} In particular, there is an enormous interest in exploiting gold colloids in (nano)biotechnology for imaging and biosensing⁴ and gene and drug delivery.⁵ However, the use of GNP in biomedical applications faces limitations like their low stability in organic fluids, the surface restrictions for binding biomolecules, and some cytotoxicity.⁶ If one could encapsulate GNP with a protecting shield, it would be possible to stabilize nanoparticles and to develop at the same time some surface functionalization. Protection of GNP from coagulation can be done conventionally by core–shell techniques, for example, by a polymer coating that usually is made of PVP or PEG.⁷ Nevertheless, the encapsulation with silica is particularly advantageous as a method for both stabilizing nanoparticles and tailoring structural and textural parameters of the outer shell, while

introducing numerous possibilities for particle functionalization.

Although some reports deal with gold colloids dispersed within a silicate matrix,⁸ encapsulation of GNP in an ordered mesoporous silica has gained great attention due to MCM-41 analogous shell properties, including highly ordered mesopores, controlled pore-size, and specific surface areas of about $1000 \text{ m}^2 \text{ g}^{-1}$. Methods like the aerosol-assisted self-assembly⁹ and the sonochemical reduction of HAuCl_4 ^{10,11} allow the confinement of gold particles (1–5 nm diameter) within the mesoporous channels of MCM-41¹⁰ or at the surface of silica spheres.¹¹ In both cases, limitations come by the non-homogeneous dispersion of the metal nanoparticles throughout the material and the impossibility to define independently the GNP diameter of the silica mesopore geometry.

As a result of the growing interest of silica nanoparticles for biological applications,¹² if one desires to take advantage of optical properties of embedded GNP it is mandatory both to trap nanoparticles of arbitrary size in a mesoporous

* To whom correspondence should be addressed. E-mail: pbotella@itq.upv.es (P.B.), acorma@itq.upv.es (A.C.). Fax: (+34) 96-387-7809. Tel.: (+34) 96-387-7800.

- (1) (a) Haruta, M.; Kobayashi, T.; Sano, H.; Yamada, N. *Chem. Lett.* **1987**, 2, 405. (b) Haruta, M.; Yamada, N.; Kobayashi, T.; Iijima, S. *J. Catal.* **1989**, 115, 301.
- (2) Daniel, M.-C.; Astruc, D. *Chem. Rev.* **2004**, 104, 293.
- (3) Corma, A.; Serna, P. *Science* **2006**, 313, 332.
- (4) Niemeyer, C. M. *Angew. Chem., Int. Ed.* **2001**, 40, 4128.
- (5) (a) Salem, A. K.; Searson, P. C.; Leong, K. W. *Nat. Mater.* **2003**, 2, 668. (b) Ow, Sullivan, M. M.; Green, J. J.; Przybycien, T. M. *Gene Ther.* **2003**, 10, 1882. (c) Pissuwan, D.; Valenzuela, S.; Cortie, M. B. *Trends Biotechnol.* **2006**, 24, 62.
- (6) (a) Vallhov, H.; Qin, J.; Johansson, S. M.; Ahlberg, N.; Muhammed, M. A.; Scheynius, A.; Gabrielsson, S. *Nano Lett.* **2006**, 6, 1682. (b) Pernodet, N.; Fang, X.; Sun, Y.; Bakhtina, A.; Ramakrishnan, A.; Sokolov, J.; Ulman, A.; Rafailovich, M. *Small* **2006**, 2, 766.
- (7) (a) Hayat, M.A. *Colloidal Gold, Principles, Methods and Applications*; Academic Press: San Diego, 1989. (b) Marinakos, S. M.; Shultz, V.; Feldheim, D. L. *Adv. Mater.* **1999**, 11, 34. (c) Gittins, D. I.; Caruso, F. *Adv. Mater.* **2000**, 12, 1947.

- (8) (a) Liz-Marzan, L. M.; Giersig, M.; Mulvaney, P. *Langmuir* **1996**, 12, 4329. (b) Mine, E.; Yamada, A.; Kobayashi, Y.; Cono, M.; Liz-Marzan, L. M. *J. Colloid Interface Sci.* **2003**, 264, 385. (c) Caruso, F. *Adv. Mater.* **2001**, 13, 11. (d) Caruso, F.; Spasova, M.; Salgueiriño-Maceira, V.; Liz-Marzan, L. M. *Adv. Mater.* **2001**, 13, 1090. (e) Chen, M. M.Y.; Katz, A. *Langmuir* **2002**, 18, 8566. (f) Lu, Y.; Yin, Y.; Li, Z.-Y.; Xia, Y. *Nano Lett.* **2002**, 2, 785. (g) Hall, S. R.; Davis, S. A.; Mann, S. *Langmuir* **2000**, 16, 1454. (h) Graf, C.; Vossen, D. L. J.; Imhof, A.; van Blaaderen, A. *Langmuir* **2003**, 19, 6693. (i) Selvan, S. T.; Nogami, M.; Nakamura, A.; Hamanaka, Y. *J. Non-Cryst. Solids* **1999**, 255, 254. (j) Budroni, G.; Corma, A. *Angew. Chem., Int. Ed.* **2006**, 45, 3328.
- (9) Lu, Y.; Fan, H.; Stump, A.; Ward, T. L.; Ricker, T.; Brinker, C. I. *Nature* **1999**, 398, 223.
- (10) Chen, W.; Cai, W.; Zhang, L.; Wang, G.; Zhang, L. *J. Colloid Interface Sci.* **2001**, 238, 291.
- (11) Pol, V. G.; Gedanken, A.; Calderro-Moreno, J. *Chem. Mater.* **2003**, 15, 1111.
- (12) Barbé, C.; Barlett, J.; Kong, L.; Finnie, K.; Lin, H. Q.; Larkin, M.; Calleja, S.; Bush, A.; Calleja, G. *Adv. Mater.* **2004**, 16, 1959.

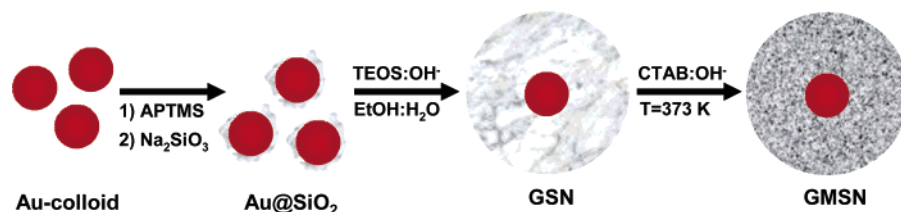


Figure 1. Sequence of GMSN synthesis through pseudomorphic synthesis.

matrix^{8a} and to control particle size of gold–mesoporous silica hybrids (i.e., 50–300 nm).¹² In this sense, Ostafin and co-workers¹³ have recently presented a liquid-phase seeded growth method using pre-existing GNP as nucleation sites for the propagation of a mesoporous shell by controlled hydrolysis of a silicon alcoxide in the presence of an organic template. Conversely to other techniques, well-ordered gold–mesoporous silica nanocomposites with diameters ranging from 150 to 450 nm are obtained by this procedure. Characteristics of this core–shell approach are the accurate control of individual particle size, pore organization, and gold occupancy (percentage of particles with at least a single gold core). A drawback of the above method is the need to optimize the simultaneous incorporation of both components of the desired silica–surfactant mesophase, as self-nucleation (formation of pure mesoporous silica nanoparticles) takes place easily. In addition, the productivity of the synthesis is severely reduced for particles lower than 200 nm in diameter, which are preferred for biological applications, and large volumes of the initial gold colloid are needed to produce small amounts of the final desired product.

Here we report the preparation and characterization of monodispersed gold–mesoporous silica nanoparticles (GMSN) ranging from 100 to 350 nm by pseudomorphical transformation^{14–18} of preformed gold–amorphous silica nanospheres (GSN) in an alkaline solution of cetyltrimethylammonium bromide (CTAB). This method allows a straightforward and fast growth of an ordered mesoporous shell endowing the GNP and minimizes self-nucleation. A scheme of the procedure is shown in Figure 1.

Experimental Section

Preparation of GNP. In a former step, a colloidal dispersion of GNP (5.0×10^{-4} M) was prepared according to the standard sodium citrate reduction method.¹⁹ A total of 500 mL of a boiling solution of hydrogen tetrachloroauric acid ($\text{HAuCl}_4 \cdot 3\text{H}_2\text{O}$) in deionized water is reduced with 3 mL of a solution of sodium citrate (1.6×10^{-3}

M). Deep-red dispersions of GNP were obtained with an average particle diameter of 15 nm or 30 nm. The absence of aggregates was confirmed by the UV–vis pattern. These colloids were used without further purification.

Synthesis of Silica-Coated GNP (Au@SiO_2). To make gold, vitreophilic 3-aminopropyltrimethoxysilane (APTMS) was bound to the surface of GNP.^{8a} A freshly prepared aqueous solution of APTMS (2.5 mL, 1 mM) was added to 500 mL of the gold solution under vigorous magnetic stirring. After 30 min, to ensure complete complexation of the amine groups with the gold surface, GNP were protected against flocculation with a thin layer of amorphous silica (Figure 1)^{8a} by introducing 20 mL of a sodium silicate solution (0.54% SiO_2) at pH = 10–11 under vigorous magnetic stirring. The resulting dispersion (pH = 8–9) was left for 48 h so that the active silica polymerized onto the gold particle surface. The silica shell thickness was about 2–4 nm. Afterward, centrifugation at 4000 rpm for 6 h is essential to remove solution with nonreacted silicate ions, avoiding further coprecipitation of silica nuclei. After centrifugation, Au@SiO_2 particles were re-dispersed in 500 mL of deionized water.

Synthesis of GSN. GSN with spherical shape were prepared by controlled growth of the silica wall in Au@SiO_2 particles in an ethanol/water mixture, according to Stober et al.'s method.²⁰ Individual particle size and gold occupancy were both controlled by the silica concentration and the introduction of ethanol as cosolvent. Typically, 80 mL of the Au@SiO_2 colloid was diluted in 400 mL of an ethanol/water mixture ($\text{EtOH}/\text{H}_2\text{O} = 2.5:1$, v/v) and 560 μL of 1 N NaOH was added under magnetic stirring. Then, 240 μL of tetraethylorthosilicate (TEOS) was introduced followed by vigorous magnetic stirring for 24 h at room temperature to allow propagation of the silica shell. Further additions of TEOS were subsequently done when required for growing of the silica wall (240 μL every 24 h, up to five additions). Finally, nanoparticles were collected by centrifugation (4000 rpm, 3 h). GSN of diameter ranging 80–350 nm with a majority (up to 70–80%) containing a single Au core were obtained. In a 48 h process (total addition of TEOS = 480 μL), the SiO_2 yield is estimated to be 80%, and the particle size distribution is 100–140 nm.

Synthesis of GMSN. GSN are used as the silica source for the synthesis of spherical GMSN by a pseudomorphic transformation.^{14–18} In a standard experiment, 0.32 g of GSN (100–140 nm) is stirred at room temperature in an alkaline solution of CTAB. The molar composition of the system is 1:0.11:0.24:395:36 $\text{SiO}_2/\text{CTAB}/\text{NaOH}/\text{H}_2\text{O}/\text{EtOH}$. After 15 min the gel is put in an autoclave in static conditions at 373 K for 0.25–24 h. The final solid is recovered by centrifugation (4000 rpm, 30 min), washed with deionized water, and dried in an oven at 323 K for 12 h. Template removal was carried out by heat treatment in the air stream at 813 K for 6 h.

Materials Characterization. Powder X-ray diffraction (XRD) patterns were collected using a Philips X'Pert diffractometer equipped with a graphite monochromator, operating at 40 kV and 45 mA and employing nickel-filtered $\text{Cu K}\alpha$ radiation ($\lambda = 0.1542$ nm).

- (13) (a) Nooney, R. I.; Dhanasekaran, T.; Chen, Y.; Josephs, R.; Ostafin, A. E. *Adv. Mater.* **2002**, *14*, 529. (b) Nooney, R. I.; Dhanasekaran, T.; Chen, Y.; Josephs, R.; Ostafin, A. E. *Langmuir* **2003**, *19*, 7628.
- (14) Martin, T.; Galarneau, A.; Di, Renzo, F.; Fajula, F.; Plee, D. *Angew. Chem., Int. Ed.* **2002**, *41*, 2590.
- (15) Pseudomorph refers to an altered mineral whose form has the outward appearance of the other mineral species from which it comes. In this case, the GMSN are pseudomorphs of the GSN.
- (16) Martin, T.; Galarneau, A.; Di, Renzo, F.; Brunel, D.; Fajula, F.; Heinisch, S.; Cretier, G.; Rocca, J.-L. *Chem. Mater.* **2004**, *16*, 1725.
- (17) (a) Pettito, C.; Galarneau, A.; Driole, M.-F.; Chiche, B.; Alonso, B.; Di, Renzo, F.; Fajula, F. *Chem. Mater.* **2005**, *17*, 2120. (b) Galarneau, A.; Iapichella, J.; Bonhomme, K.; Di, Renzo, F.; Kooyman, P.; Terasaki, O.; Fajula, F. *Adv. Funct. Mater.* **2006**, *16*, 1657.
- (18) Lim, S.; Ranade, A.; Du, G.; Pfefferle, L. D.; Haller, G. L. *Chem. Mater.* **2006**, *18*, 5584.
- (19) (a) Enüstün, B. V.; Turkevich, J. *J. Am. Chem. Soc.* **1963**, *85*, 3317. (b) Frens, G. *Nature Phys. Sci.* **1973**, *241*, 20.

- (20) Stober, W.; Fink, A.; Bohn, E. *J. Colloid Interface Sci.* **1968**, *26*, 62.

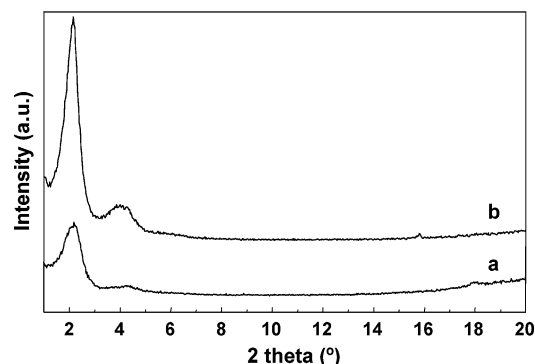


Figure 2. XRD patterns of core-shell gold-silica nanoparticles: (a) as-made GMSN and (b) calcinated (air, 540 °C) GMSN.

Table 1. Compositional and Structural Characteristics of As-Synthesized Gold-Silica Nanoparticles Prepared by Stober's Method and Pseudomorphic Synthesis at Different Times^a

sample	time (h)	Au (wt %)	<i>d</i> -spacing (Å)	<i>Y</i> _{SiO₂} (wt %)	<i>Y</i> _{CTMA} ^b (wt %)	CTMA/SiO ₂ (M)
GSN	0	10.6		80		
GMSN-0.25	0.25	10.7	37	49	63	0.143
GMSN-1	1	6.9	38	73	90	0.137
GMSN-2	2	8.5	38	62	87	0.132
GMSN-4	4	8.9	38	78	86	0.127
GMSN-24	24	10.8	38	74	85	0.128

^a Pseudomorphic transformation conditions, *T* = 373 K; gel molar composition, 1:0.11:0.24:395:36 SiO₂/CTAB/NaOH/H₂O/EtOH. ^b Calculated from carbon analysis.

Liquid nitrogen adsorption isotherms of 200 mg of sample were measured in a Micromeritics Flowsorb apparatus. Surface area calculations were carried out using the BET method, whereas the pore size distribution was calculated according to the Kruk-Jaroniec-Sayari estimation.²¹

NMR spectra were recorded at room temperature under magic angle spinning (MAS) on a Bruker AV400 spectrometer. The single pulse ²⁹Si spectra were acquired using pulses of 3.5 μs corresponding to a flip angle of 3π/4 rad and a recycle delay of 240 s. The ¹H to ¹³C cross-polarization (CP) spectra were acquired by using a 90° pulse for ¹H of 5 μs, a contact time of 5 ms, and a recycle of 3 s. All spectra were recorded with a 7 mm Bruker BL-7 probe and at sample spinning rate of 5 kHz. The ²⁹Si spectra were referenced to tetramethylsilane (TMS) and the ¹³C to adamantane.

Samples for transmission electron microscopy (TEM) were ultrasonically dispersed in 2-propanol and transferred to carbon coated copper grids. TEM micrographs were collected in a Philips CM-10 microscope operating at 100 kV.

Finally, carbon percentage in surfactant-containing samples was measured by elemental analysis (FISONS, EA 1108 CHNS-O), and gold content in calcinated GMSN was determined by X-ray fluorescence (Philips MiniPal 25 fm spectrometer).

Results and Discussion

The recovered solid after the hydrothermal treatment presents an XRD pattern of MCM-41^{22a} (Figure 2a) with the same morphology of the parent amorphous silica and

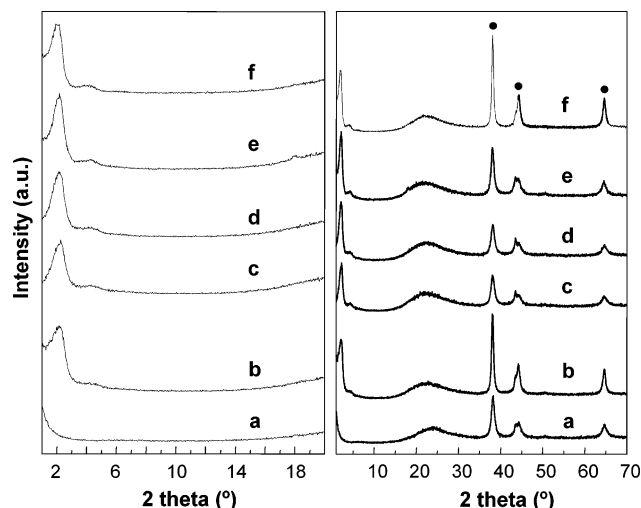


Figure 3. XRD patterns of as-synthesized GMSN samples at *T* = 373 K within time (0.25–24 h): (a) *t* = 0 h; (b) *t* = 0.25 h; (c) *t* = 1 h; (d) *t* = 2 h; (e) *t* = 4 h; and (f) *t* = 24 h. Besides the reflections corresponding to the hexagonal symmetry peaks corresponding to GNP (●) can be seen.

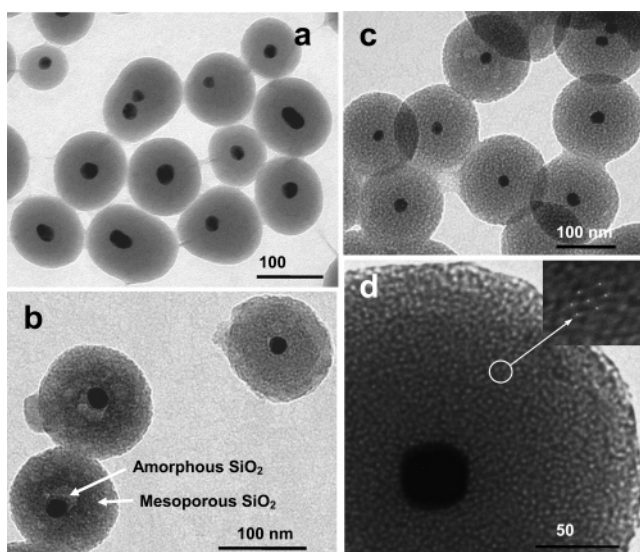


Figure 4. (a) GSN prepared by Stober's method; (b, c) GMSN synthesis by pseudomorphic transformation of preformed GSN at an intermediate state detected at *t* = 15 min (b) and after complete change (c); and (d) detail of wormhole-like channels of GMSN microstructure; the inset shows the local arrangement in hexagonal symmetry.

similar particle size distribution, containing the GNP inside. A main diffraction peak at *d*-spacing of *d*₁₀₀ = 38 Å is indexed according to a hexagonal cell with *a* = 44 Å, typical of MCM-41 materials. However, secondary reflexions of MCM-41 (indexed as (110) and (200)) overlap in a broad band. This is not surprising, taking into account that the spherical shape of MCM-41 sub-micrometer particles limits the pore ordering in a large scale, distorting the hexagonal symmetry and giving rise to broader lines in the XRD pattern.²²

The transformation of the parent silica in the mesoporous structure takes place in only 15 min, and no further phase change was observed even when the synthesis was prolonged for 24 h (Table 1, Figure 3). The fraction of incorporated surfactant increases with time up to 90% in the first hour and remains stable (see Table 1). The structural integrity was

(21) Kruk, M.; Jaroniec, M.; Sayari, A. *Langmuir* **1997**, *13*, 6267.

(22) (a) Schacht, S.; Janicke, M.; Schüth, F. *Microporous Mesoporous Mater.* **1998**, *22*, 485. (b) Pauwels, B.; Van Tendeloo, G.; Thoenen, C.; Van Rhijn, W.; Jacobs, P. A. *Adv. Mater.* **2001**, *13*, 1317. (c) Liu, S.; Cool, P.; Collart, O.; Van Der Voort, P.; Vansant, F. E.; Lebedev, O. I.; Van Tendeloo, G.; Jiang, M. *J. Phys. Chem. B* **2003**, *107*, 10405. (d) Tan, B.; Rankin, S. E. *J. Phys. Chem. B* **2004**, *108*, 20122.

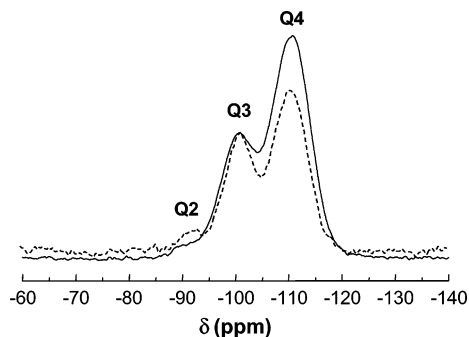


Figure 5. ^{29}Si MAS NMR spectra of as-synthesized core-shell gold-silica nanoparticles prepared by Stober's method (GSN, solid line) and pseudomorphic synthesis ($T = 373$ K, $t = 4$ h, sample GMSN-4, dashed line).

retained after the removal of surfactant by calcination at 813 K (Figure 2b), supporting the stability of the mesoporous silica shell.

TEM images show clearly that GMSN retain the shape of the preformed spheres and keep similar size distribution (Figure 4). This suggests that the micelle-templated system is created through progressive dissolution of amorphous silica by the alkaline solution and interaction with the surfactant (Figure 4b). After the hydrothermal treatment, formed GMSN reveal a quite complex pore structure, where the mesochannels do not align over the entire nanoparticle but form wormhole-like pores that are randomly distributed in all directions, starting at the inner part of the sphere and going out to the external edge (Figure 4d). Nevertheless, the hexagonal symmetry is easily recognizable in the mesoporous wall at small domains (Figure 4d, inset). Working at the standard synthesis conditions, we obtain a narrow particle size distribution of 110–150 nm.

In the development of a micelle templated system from an amorphous precursor the degree of condensation of the silicate framework can be affected. The ^{29}Si MAS NMR spectrum of GSN shows a high degree of silica polymerization with typical resonances at -92 , -101 , and -111 ppm, which are assigned to Q_2 ($[\text{Si}(\text{OSi})_2(\text{OH})_2]$), Q_3 ($[\text{Si}(\text{OSi})_3(\text{OH})]$), and Q_4 ($[\text{Si}(\text{OSi})_4]$) species, respectively (Figure 5).²³ Deconvolution of the NMR signals led to 2% Q_2 , 32% Q_3 , and 65% Q_4 . Conversely, after the pseudomorphic transformation a slight increase in the concentration of silanol groups is observed with Q_2 , Q_3 , and Q_4 values of 6, 35, and 59%, respectively. While it is true that the differences are rather small, because of the reproducibility of the results we have included such observation. If we accept these differences are real, they would be in good correspondence with MCM-41 material obtained by pseudomorphic synthesis in low alkaline media ($\text{OH}^-/\text{SiO}_2 = 0.25$),¹⁴ which presents about 60–70% of siloxane groups. As was said before, no phase transformation takes place after formation of GMSN, even if the synthesis is taken to extreme conditions like long synthesis time (i.e., 1 week) or higher pH (i.e., $\text{OH}^-/\text{SiO}_2 = 0.35$ – 0.75). The high degree of silica condensation achieved in our synthetic conditions for the GMSN limits the possibility

Table 2. Textural Characteristics of Gold-Silica Nanoparticles Prepared by Stober's Method and Pseudomorphic Synthesis

sample	sphere average diameter (nm)	unit cell (Å)	V_p^b ($\text{cm}^3 \text{g}^{-1}$)	S_{BET}^c ($\text{m}^2 \text{g}^{-1}$)	D^d (Å)	t^e (Å)
GSN	100–140		0.07	34		
GMSN-4 ^a	110–150	44	0.65	1020	35	9

^a Pseudomorphic transformation conditions, $T = 373$ K; gel molar composition, 1:0.11:0.24:395:36 $\text{SiO}_2/\text{CTAB}/\text{NaOH}/\text{H}_2\text{O}/\text{EtOH}$. ^b Pore volume. Value corrected for the pure silica sample. ^c Surface area. Value corrected for the pure silica sample. ^d Pore diameter. Calculated according to the Kruk-Jaroniec-Sayari (KJS) method.²¹ ^e Wall thickness.

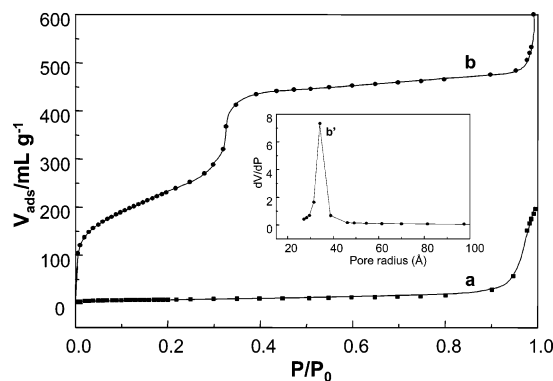


Figure 6. BET nitrogen adsorption isotherms of GSN (a) and GMSN-4 (b) samples and pore size distribution of the mesoporous material (inset).

of any phase transition as could be expected with other less polymerized materials obtained by pseudomorphic synthesis.¹⁷

The adsorption pattern obtained from the nitrogen isotherms for the precursor GSN corresponds to a nonporous silica with very low external surface area ($34 \text{ m}^2 \text{g}^{-1}$) and pore volume ($0.07 \text{ cm}^3 \text{g}^{-1}$; Table 2, Figure 6). During the hydrothermal treatment, the incorporation of CTAB to the amorphous silica matrix leads to a mesostructured material that after calcination gives a surface area of $1020 \text{ m}^2 \text{g}^{-1}$ with no modification of the particle shape and size, obtaining monodispersed spherical GMSN (Table 2, Figure 4c). The sample GMSN-4 presents an adsorption isotherm type IV typical of MCM-41 type materials with a sharp inflection at the point of capillary condensation around $p/p_0 = 0.36$ (see Figure 4). The average pore diameter is 35 Å according to the Kruk-Jaroniec-Sayari (KJS) method,²¹ and no secondary porosity was observed in the pseudomorphically transformed solid. Moreover, due to the low surface area of preformed GSN the kinetics of silica dissolution in alkaline medium is slow, which allows simultaneous incorporation of the surfactant and avoids the formation of new gold-free MCM-41 nanoparticles (see Figure 4).

Conclusions

We have synthesized by a simple and fast method nanosized gold-mesoporous silica hybrids by pseudomorphic transformation of preformed GSN. In an optimized procedure, monodispersed, uniform nanoparticles ranging 100–350 nm and $1000 \text{ m}^2 \text{g}^{-1}$ surface area with a centered metal core of about 15 or 30 nm and high gold occupancy are prepared. The abundant silanol groups present on the surface offer an exceptional support for particle functional-

(23) (a) Chen, C. Y.; Li, H. X.; Davis, M. E. *Microporous Mater.* **1993**, *2*, 17. (b) Chen, C. Y.; Li, H. X.; Davis, M. E. *Microporous Mater.* **1993**, *2*, 27.

ization while the mesoporous structure allows confining and controlled diffusion of molecules and GNP give optical properties to these composites. These features make these nanohybrids potential vehicles for drug and gene delivery, quantum-dot technology, and biosensing. We think that this technology can also be extended to other metal–mesoporous silica nanoparticles with variable quantum-size effects.

Acknowledgment. The authors thank CICYT (MAT2006-14274-C02-01) and Generalitat Valenciana (GV05/173) for financial support and the Electronic Microscopy Service of UPV for technical support. P.B. also thanks the program Ramón y Cajal of Spain.

CM0629457